SAND79-7023
Unlimited Release
UC-62 Distribution
Prepared for Sandia Laboratories
under Contract No. 13-5164

Analysis of Field Test Results for Single-Axis Tracking Solar Collector Foundations

H.E. Auld

Higgins, Auld, & Associates

Prepared by Sandia Laboratories, Albuquerque, New Mexico 87185
and Livermore, California 94550 for the United States Department
of Energy under Contract DE-AC04-76DP00789

July 1979

Sandia National Laboratories

Issued by Sandia Laboratories, operated for the United States Department of Energy by Sandia Corporation.

Printed in the United States of America

Available from
National Technical Information Service
U.S. Department of Commerce
5285 Port Royal Road
Springfield, VA 22161

Price: Printed Copy $4.50; Microfiche $3.00

SAND79-7023 Distribution
Unlimited Release Category UC-62
Printed July 1979

ANALYSIS OF FIELD TEST RESULTS FOR SINGLE-AXIS-TRACKING SOLAR COLLECTOR FOUNDATIONS

Harry E. Auld

Higgins, Auld & Associates
2601 Wyoming Boulevard, N.E., Suite H-1
Albuquerque, New Mexico 87112

ABSTRACT

Five reinforced concrete cylindrical piers, typical of foundations utilized for single-axis-tracking solar collector systems, were tested to determine eccentric horizontal and vertical failure loads. The results from these tests were found to compare favorably with the results from theoretical calculations which incorporate the geotechnical parameters of the test site. Recommendations are made for the incorporation of these results into the design of foundations for future solar collector systems.

CONTENTS

ILLUSTRATIONS

TABLES

SECTION I

INTRODUCTION

Single-axis-tracking solar collector systems are normally supported by rows of pedestals which rest on reinforced concrete cylindrical pier foundations (see figure 1). The Department of Energy's solar irrigation project in Estancia Valley, near Albuquerque, New Mexico is a typical example of such an installation in use today. The pier foundations for these systems are relatively expensive and they result in a significant percentage of the overall cost of the collector field. Therefore, Sandia Laboratories has funded studies to attempt to minimize foundation costs for future systems (refs. 1 and 2).

Reference 1 studied several alternate foundation concepts and concluded that the reinforced concrete cylindrical pier is the most economical design and should be utilized whenever site conditions permit their construction. This study also indicated that the aerodynamic wind loads which have been used may be somewhat over conservative and that the full strength of the insitu soil may not have been included in foundation designs. Therefore, a standardized design procedure for reinforced concrete cylindrical pier foundations was developed.

Reference 3 presents a standardized procedure for estimating the aerodynamic loads on a typical single-axis-tracking solar collector system. The loads obtained from this procedure are very similar to those previously reported in reference 1. In addition, reference 3 indicated that shielding effects from both the presence of multiple collector rows and perimeter fencing could result in significant wind load reductions.

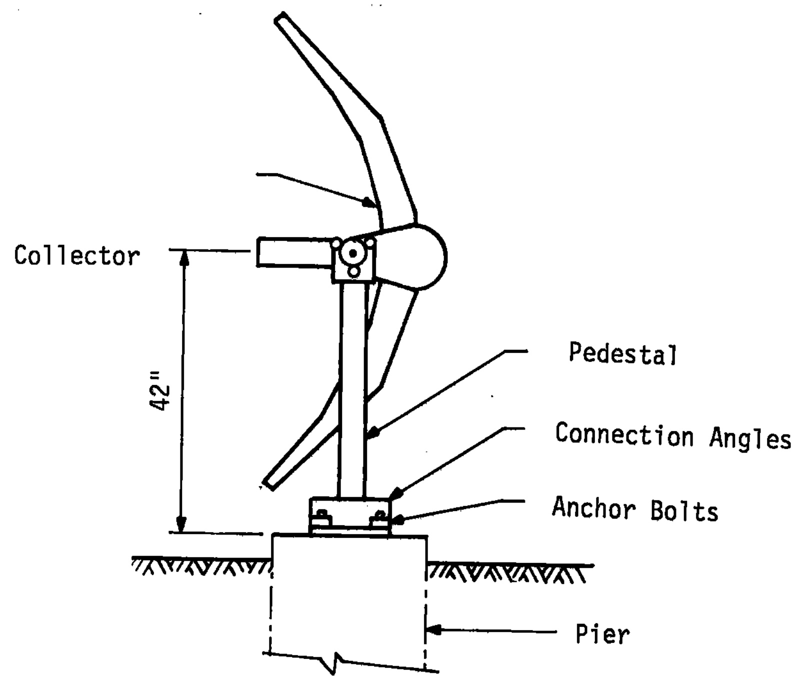

Figure 1. Typical Single-Axis-Tracking Solar Collector System Installation

Reference 2 studied the implications of reduced loading conditions on foundation designs.

Because these studies indicated that the size of foundations could be reduced for future systems, Sandia Laboratories undertook a foundation test program. The objectives of this program were to obtain field test results on the strength of typical foundation installations and to provide data for the evaluation of the analytical design procedures developed in reference 1, thereby providing increased confidence for the design of future systems. This report documents the results of the foundation test program conducted by Sandia Laboratories on May 15, 1979.

SECTION II

SUMMARY OF TEST CONDITIONS

1. CONSTRUCTION DETAILS

The test site was located in Sandia Laboratories' Solar Collector Test Area, just south of F Street on Kirtland Air Force Base, New Mexico. Five reinforced concrete cylindrical pier foundations were constructed as shown in figure 2. The piers were numbered consecutively, from east to west. Table 1 provides data on the pier dimensions and number of anchor bolts. The piers were constructed in drilled uncased holes utilizing 3000 psi concrete, grade 40 reinforcing steel, and A307 steel anchor bolts. Figure 3 depicts a typical 12 inch diameter pier and figure 4 depicts a typical 18 inch diameter pier. Figure 5 illustrates the general configuration of the anchor bolt placement. The piers were constructed approximately 60 days prior to the test date.

TABLE 1. PIER CHARACTERISTICS

Pier Number*	1	2	3	4	5
Diameter, inch	12	18	18	12	12
Length, feet-inch	4-6	6-5	7-5	5-6	7-3
Number of Anchor Bolts**	2	4	4	1	2

* See figure 2 for site plan

** See figure 5 for anchor bolt placement

2. GEOTECHNICAL PARAMETERS

Two ten foot deep soil investigation holes were drilled in line with

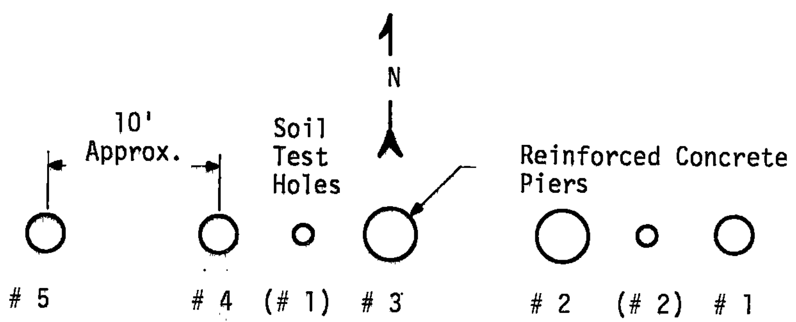

Figure 2. Site Plan of Test Area

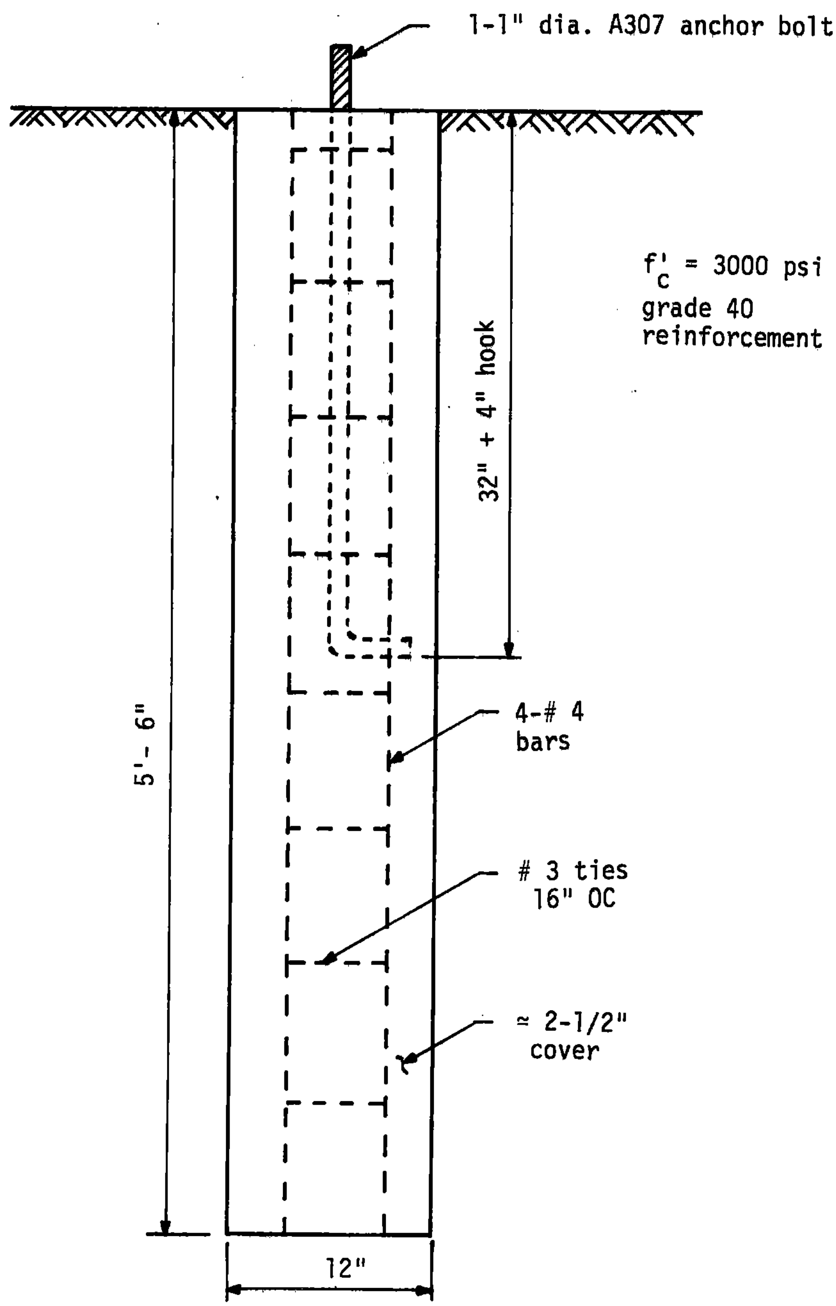

Figure 3. Typical 12" Diameter Pier (#4)

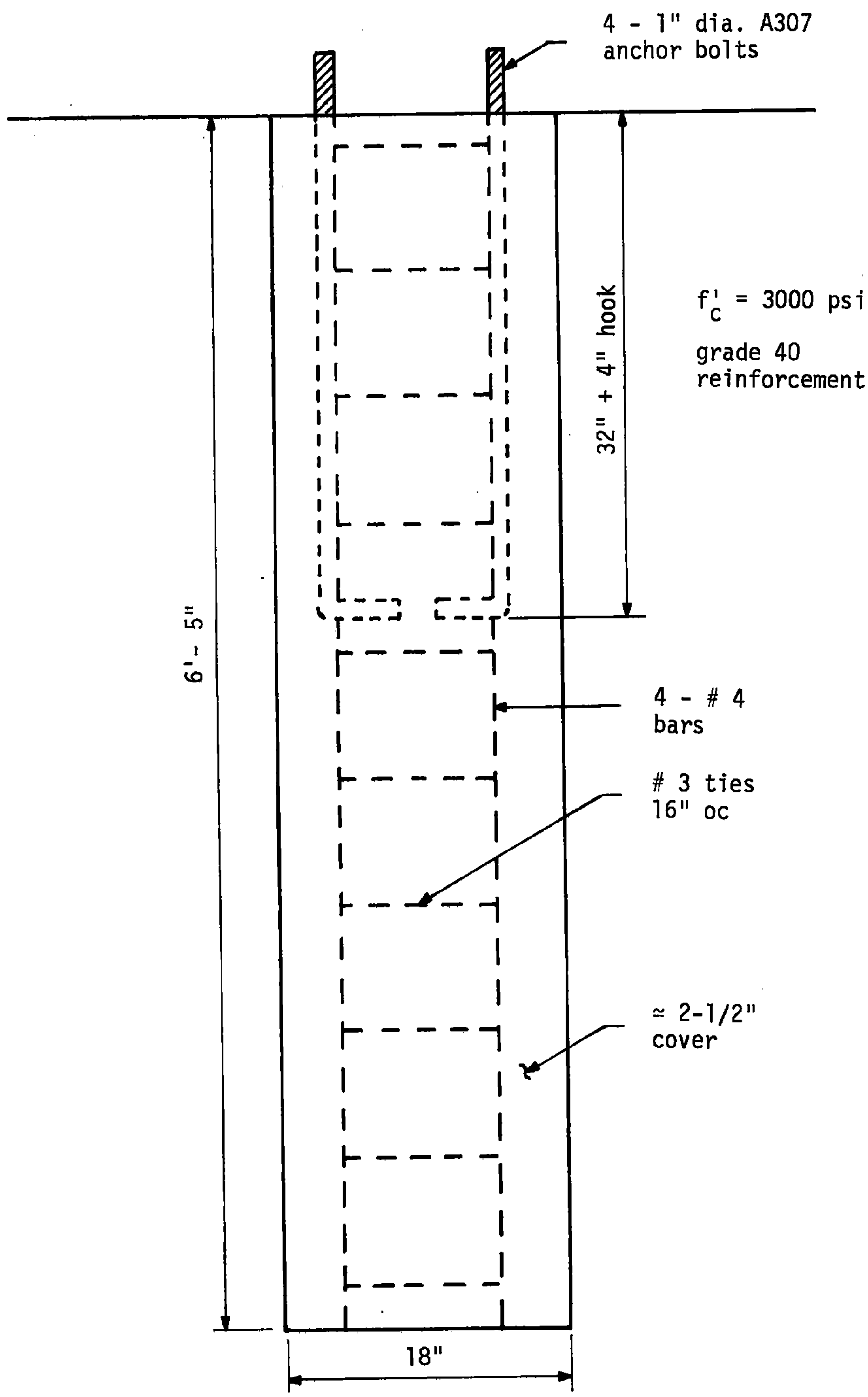

Figure 4. Typical 18" Diameter Pier (#2)

8

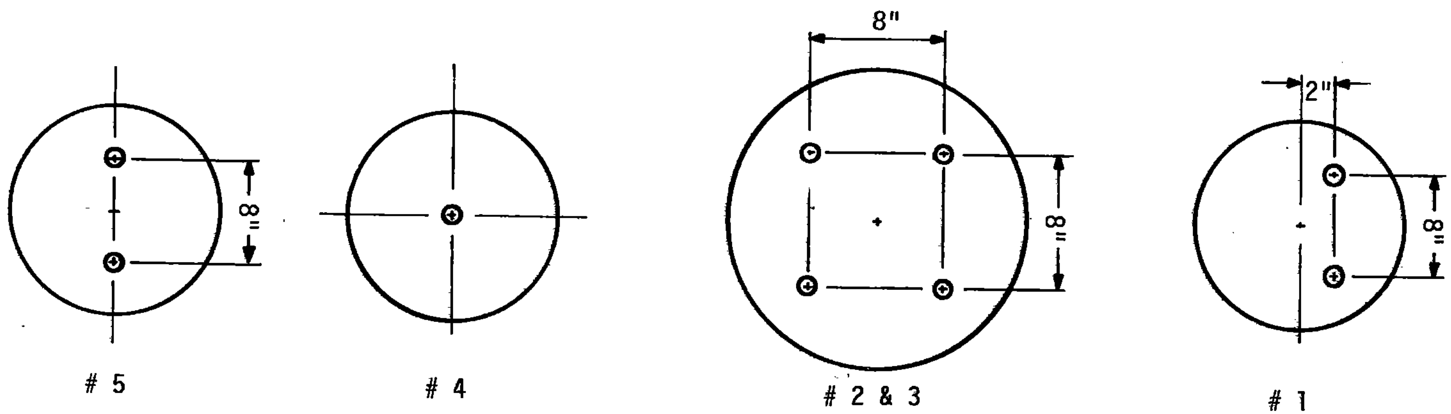

Figure 5. Anchor Bolt Placement

the test piers, as shown in figure 2. The logs from these borings are shown in figure 6. The material to a depth of seven feet can generally be described as a medium plastic, sandy clay with properties as given in table 2.

TABLE 2. SOIL PROPERTIES

Dry Density pcf	Moisture Content %	Atterberg Limits LL	PI
103	14	35	16

The observed average standard penetration resistance of ten blows per foot, to a depth of seven feet, correlates with an angle of internal friction of approximately 30 degrees for a cohesionless soil or an unconfined compressive strength of approximately 1-1/4 tons per square foot for a cohesive soil (ref. 4). These correlations are in reasonable agreement with the results obtained from direct shear tests on undisturbed samples, which indicate an angle of internal friction of approximately 35 degrees and a cohesion value of approximately 1500 pounds per square foot (ref. 5). Based upon reference 1, this site would fall approximately midway between the classification of a poor site and a typical site.

3. TEST PROCEDURES

Two test frames were fabricated to permit the application of horizontal loads 42 inches above the base plate and vertical loads through the center of gravity of the anchor bolt pattern. The loads were applied with a hydraulic jack, utilizing a forklift as the reaction weight. Loads were measured with a load cell which had a maximum capacity of approximately 20,000 pounds. Displacements were measured utilizing a transit. Figure 7 is a photograph of one of the test frames being prepared for the application of a horizontal load.

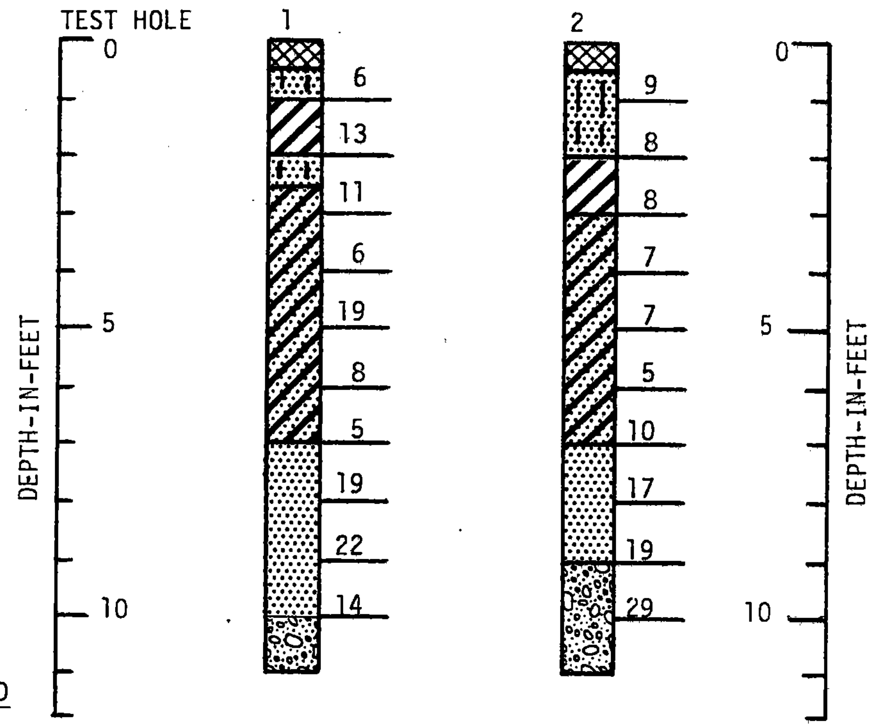

LEGEND

ASPHALTIC PAVEMENT

SAND, coarse to fine, silty, loose, slightly moist, calcareous, brown (SM)

CLAY, lean, slightly sandy, moderately silty, medium stiff, slightly moist, very calcareous, light brown mottled with buff (CL)

CLAY, lean, sandy (fine), silty, medium stiff to very stiff, slightly moist, calcareous, brown (CL)

SAND, coarse to fine, slightly silty to silty, traces of clay and gravel, medium dense, dry, calcareous, brown to dark gray (SP-SM)

SAND AND GRAVEL, traces of silt and clay, medium dense to dense, dry, calcareous, brown to dark gray (SP-GP)

NOTES

1. (6) indicates location of Penetration Resistance Tests and number of blows with a 140-pound hammer, falling 30 inches, required to drive the sampler 12 inches.

Figure 6. Soil Boring Logs

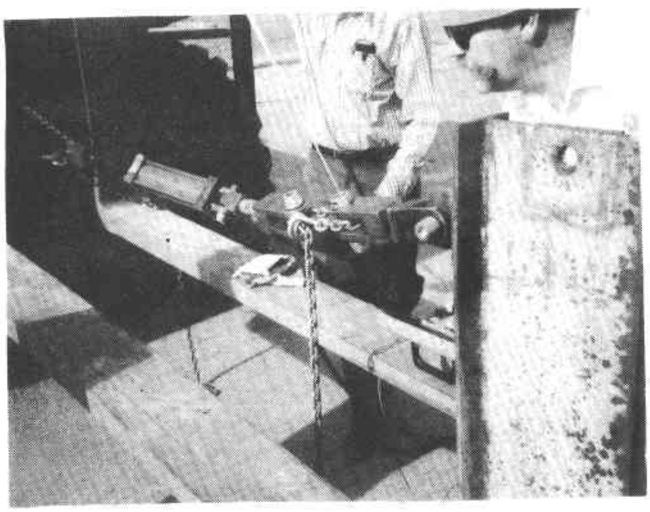

Figure 7. Preparing to Apply Horizontal Load to Heavy Duty Test Frame

A heavy duty test frame fabricated from a S 12 x 35 structural steel member was utilized to apply the loads to the 18 inch diameter piers (# 2 and 3). The standard pedestal, which is fabricated from 4 inch x 4 inch x 1/4 inch square structural tubing, was utilized to apply the loads to the 12 inch diameter piers (# 1, 4 and 5).

The number of anchor bolts provided was varied to permit the evaluation of various options for connecting the pedestal to the pier foundations. Piers # 2 and 3 each had four anchor bolts and are typical of current field installations. A one inch thick rectangular steel plate, welded to the bottom of the heavy duty test frame, was utilized to connect the test frame to the pier anchor bolts. Leveling nuts were installed under the plate and both washers and nuts were installed above the plate, as shown in the photograph in figure 8. Note that the asphalt pavement has been removed (approximately 3 foot x 3 foot square) to minimize its effect on the test results.

The remaining piers had less than four anchor bolts (either one or two). A 3/8 inch thick adaptor plate was utilized to connect the 4 inch x 4 inch x 3/8 inch angles, welded to the base of the pedestal, to the anchor bolts. The tops of these piers were grouted to provide a level surface. The adaptor plate was then fastened to the anchor bolts utilizing leveling nuts under the plate. Four each one inch diameter A307 bolts were then installed through the angles and the adaptor plate and positioned to provide equal bearing against the grout surface. These four bolts (outriggers) were utilized to provide additional bearing and thereby stiffen the connection. Figure 9 is a photograph of this connection installed on pier # 1. Note that the pier in this photograph has already failed under the application of both the horizontal and vertical loads.

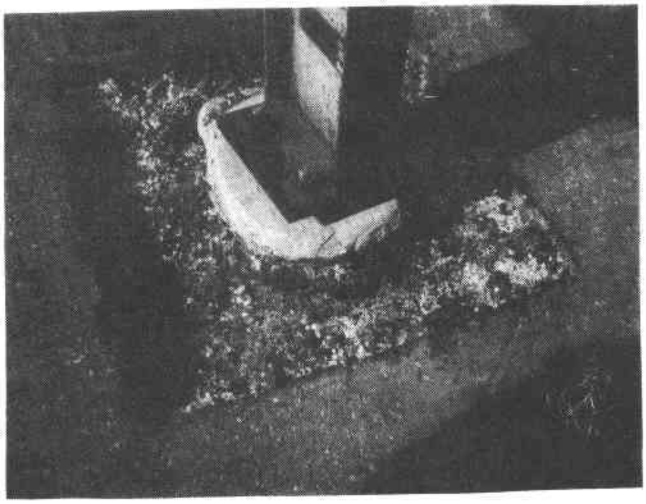

Figure 8. Heavy Duty Test Frame Installed on Pier # 2

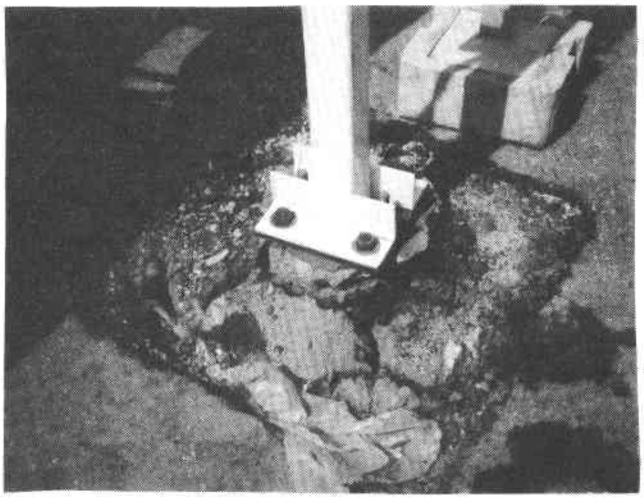

Figure 9. Standard Pedestal Test Frame Installed on Pier # 1

In each test, the horizontal load was applied first. The load was applied in uniform increments and the test frame was allowed to reach displacement equilibrium prior to applying the next increment of load. An unload-load cycle was applied when the load reached approximately 1/3 to 1/2 of the predicted failure load. When the apparent failure load was reached, deflections were measured for 30 second intervals to give an indication of time rate effects.

The vertical load was applied in a similar manner, after failure was achieved from the application of the horizontal load. However, hysterisis loops were not obtained during the vertical loading cycle. In some cases, the maximum vertical load was limited by the capacity of the load cell. After reaching either failure or the capacity of the load cell, the load cell was disconnected and the forklift was used to remove the pier from the ground. Because of space restrictions from nearby solar collectors, pier # 5 was not tested with vertical loads or removed from the ground.

SECTION III

TEST RESULTS

Horizontal load-displacement curves were obtained for each pier/test frame unit. It was obvious from the test results that the standard pedestal test frame (4 inch x 4 inch x 1/4 inch square post with connection angles) was much more flexible than the rigid boundary conditions assumed for prediction calculations. Therefore, this test frame was loaded in the laboratory with conditions approximating those utilized in the field test. A horizontal load-displacement curve for the standard pedestal test frame is shown in figure 10. The frame remains elastic until a load of approximately six kips.

Figures 11 through 14 present the horizontal load-displacement curves for piers # 1, 2, 3 and 5. The curves for piers # 1 and 5 have been corrected to remove the displacements resulting from the standard pedestal test frame flexibility. The displacements remaining after these corrections have been made should result from pier rotation. The horizontal load-displacement curve for pier # 4 is not shown. Excessive horizontal displacements of the test frame were observed under small increments of load. Since the single anchor bolt was incapable of transmitting the applied load to the pier foundation, the horizontal load test was discontinued.

Figure 15 presents a summary of the vertical load-displacement curves. No vertical load test was conducted on pier # 5, as previously explained. The results for pier # 4 appear to contain an anomoly. Post-test inspection of the apparatus for this test revealed that there was a bearing failure in the area of the adaptor plate/washer.

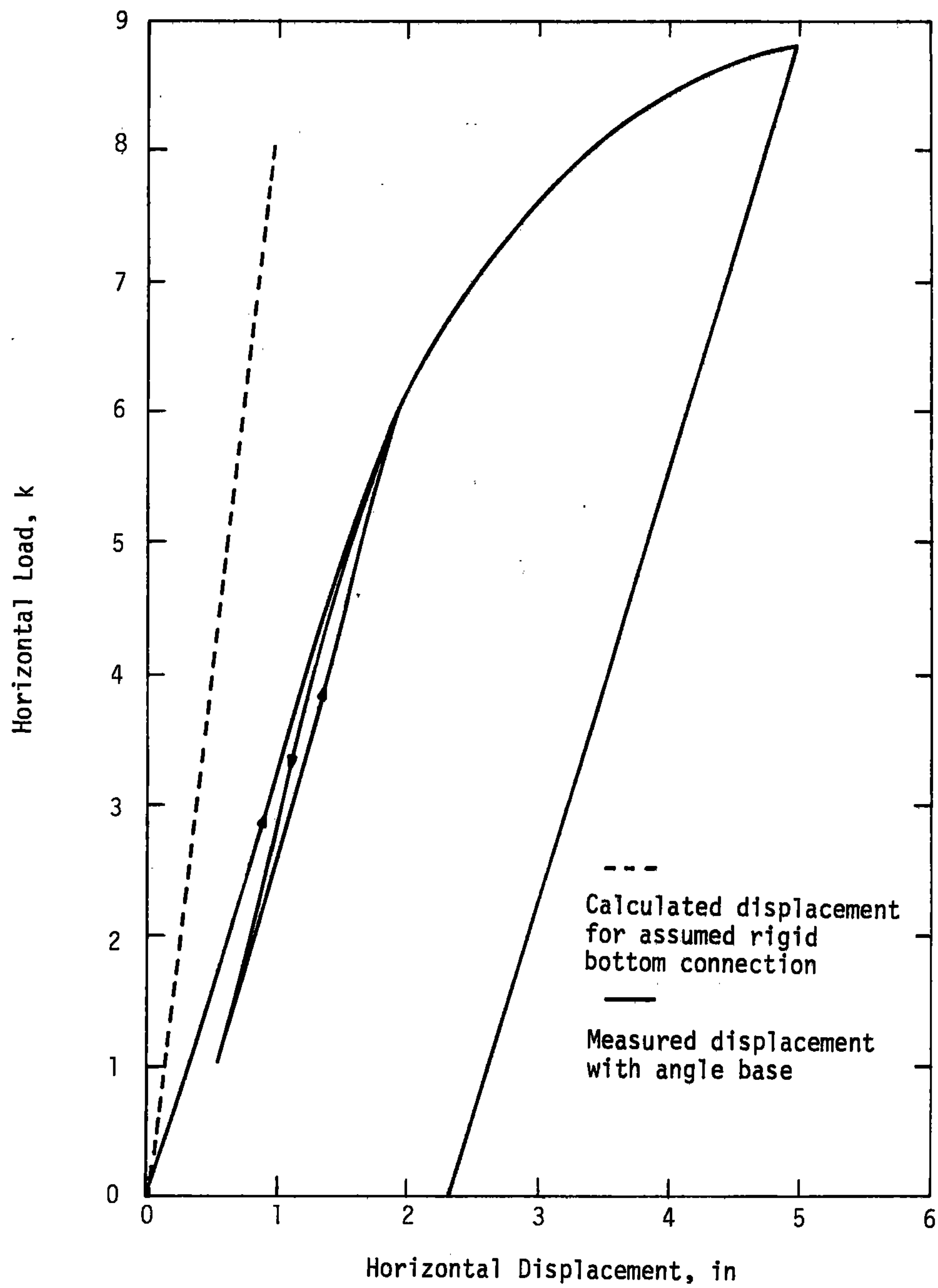

Figure 10. Horizontal Load-Displacement Curve, 4" x 4" x 1/4" Square Post

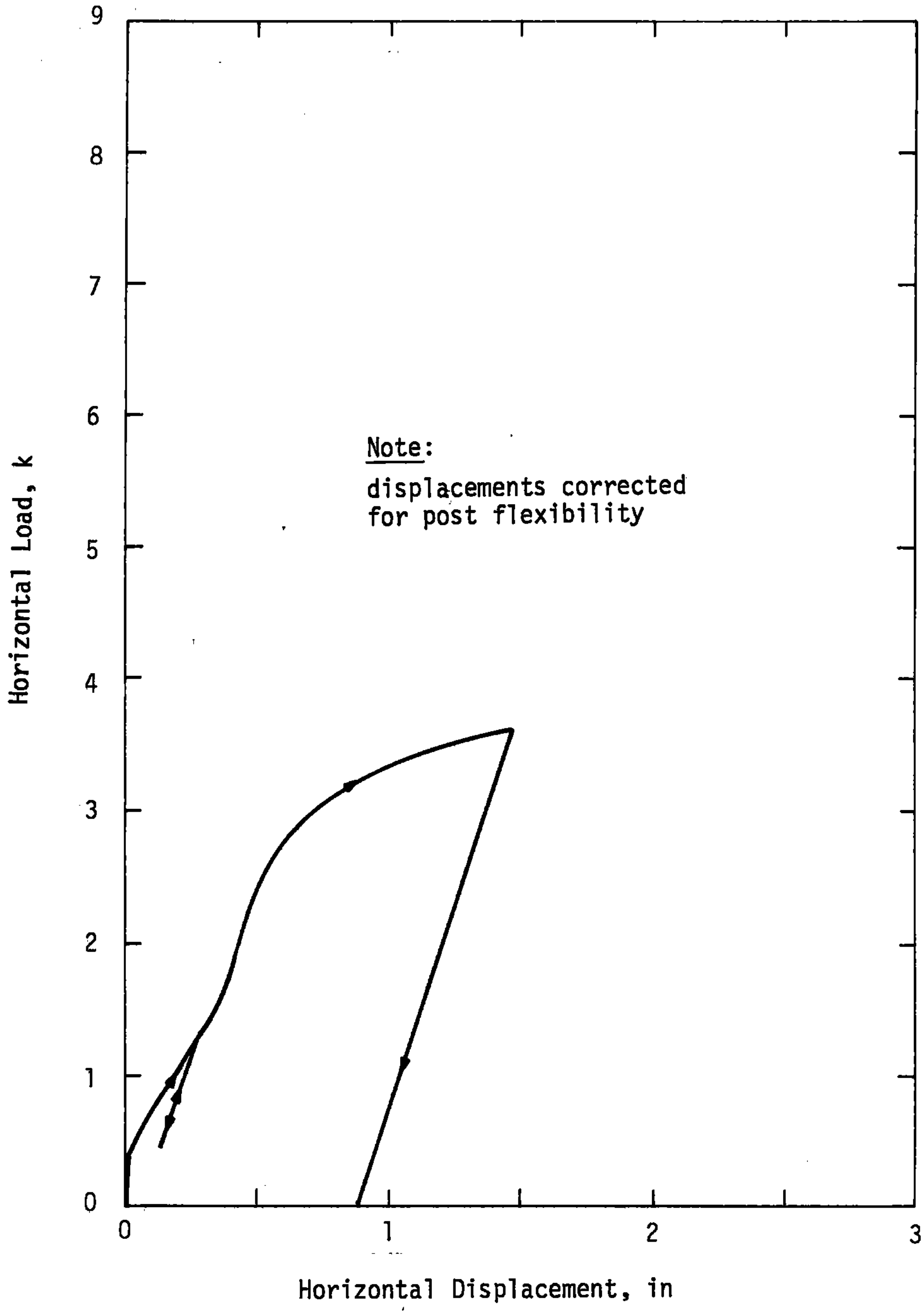

Figure 11. Horizontal Load-Displacement Curve, Pier # 1

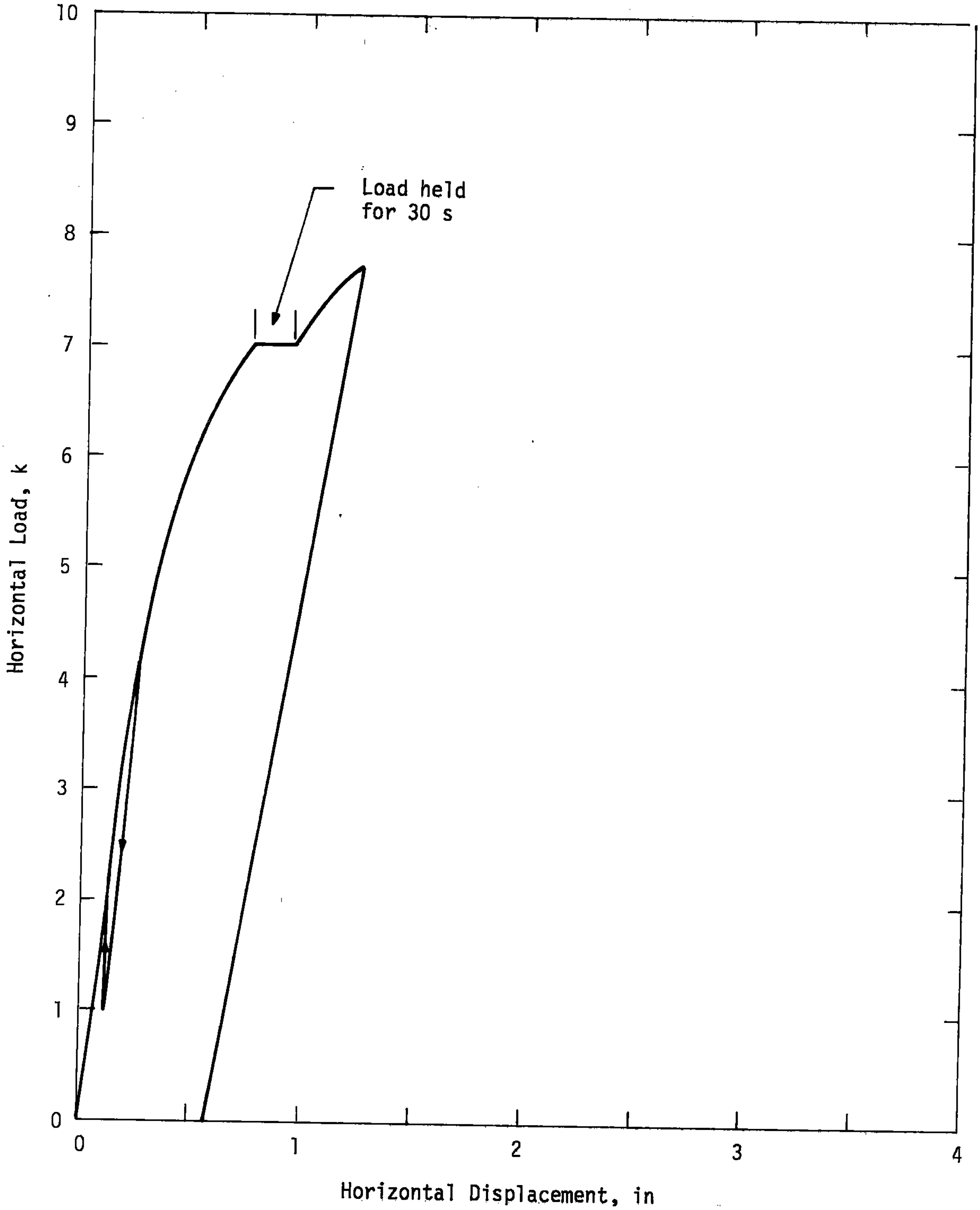

Figure 12. Horizontal Load-Displacement Curve, Pier # 2

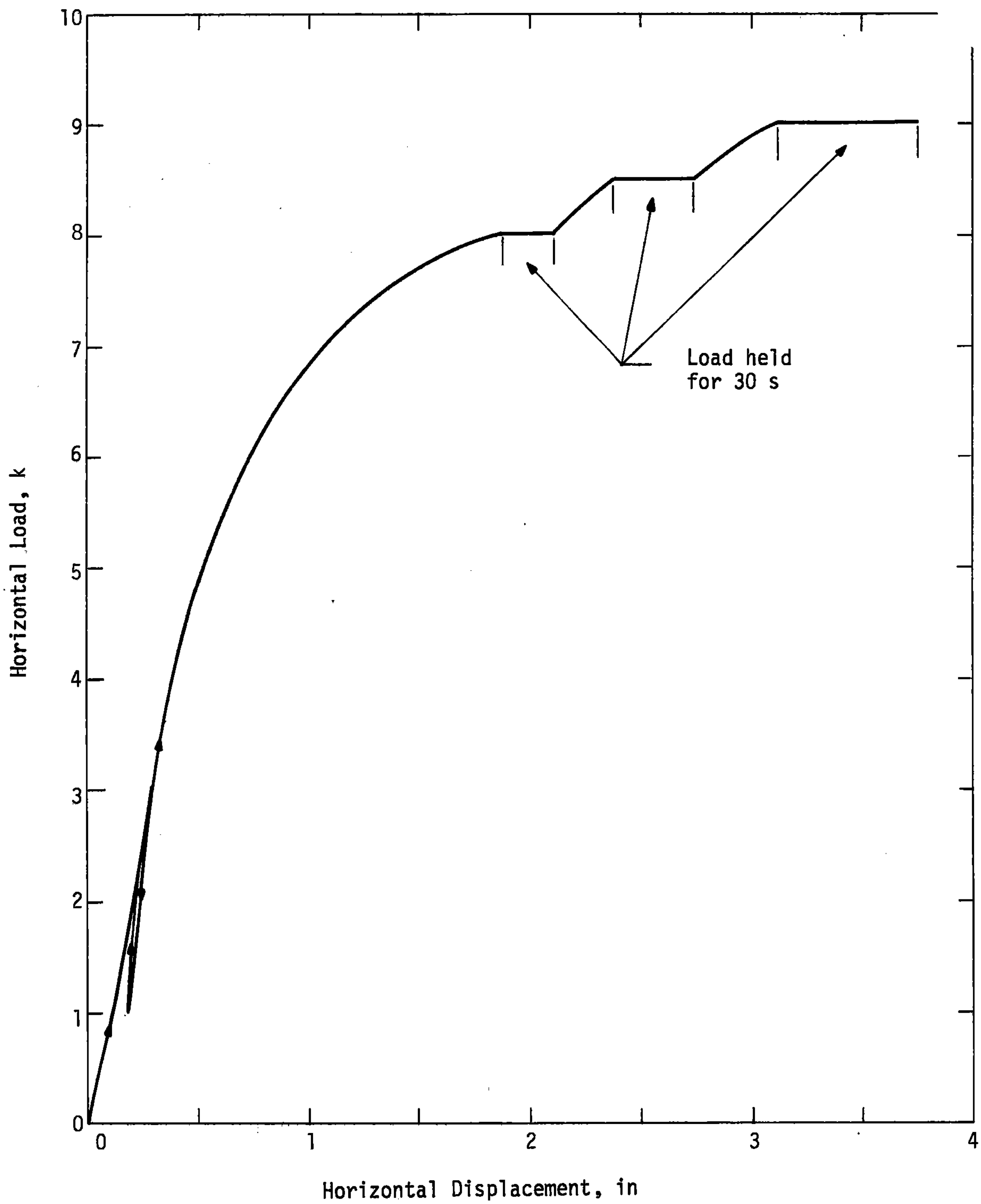

Figure 13. Horizontal Load-Displacement Curve, Pier # 3

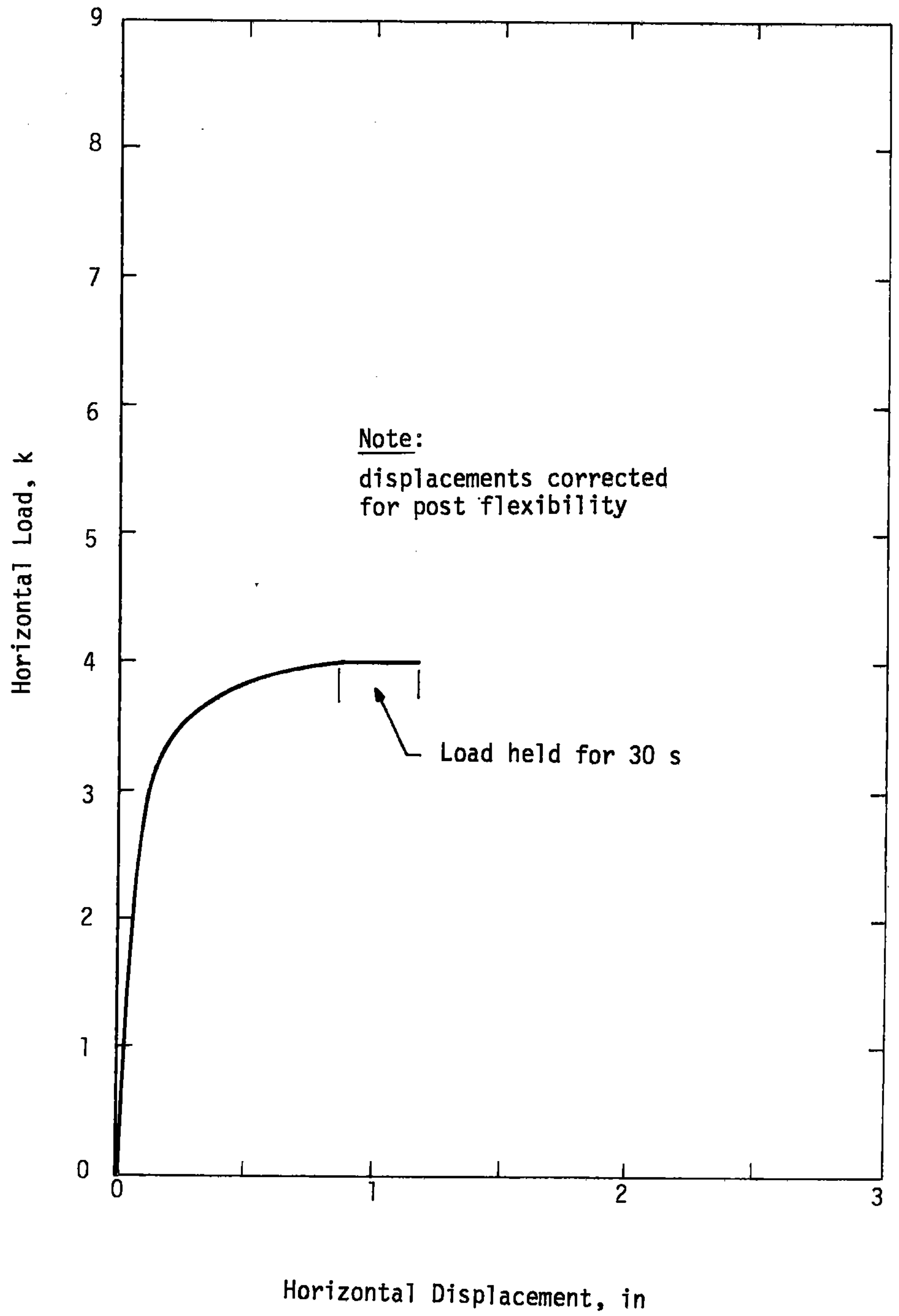

Figure 14. Horizontal Load-Displacement Curves, Pier # 5

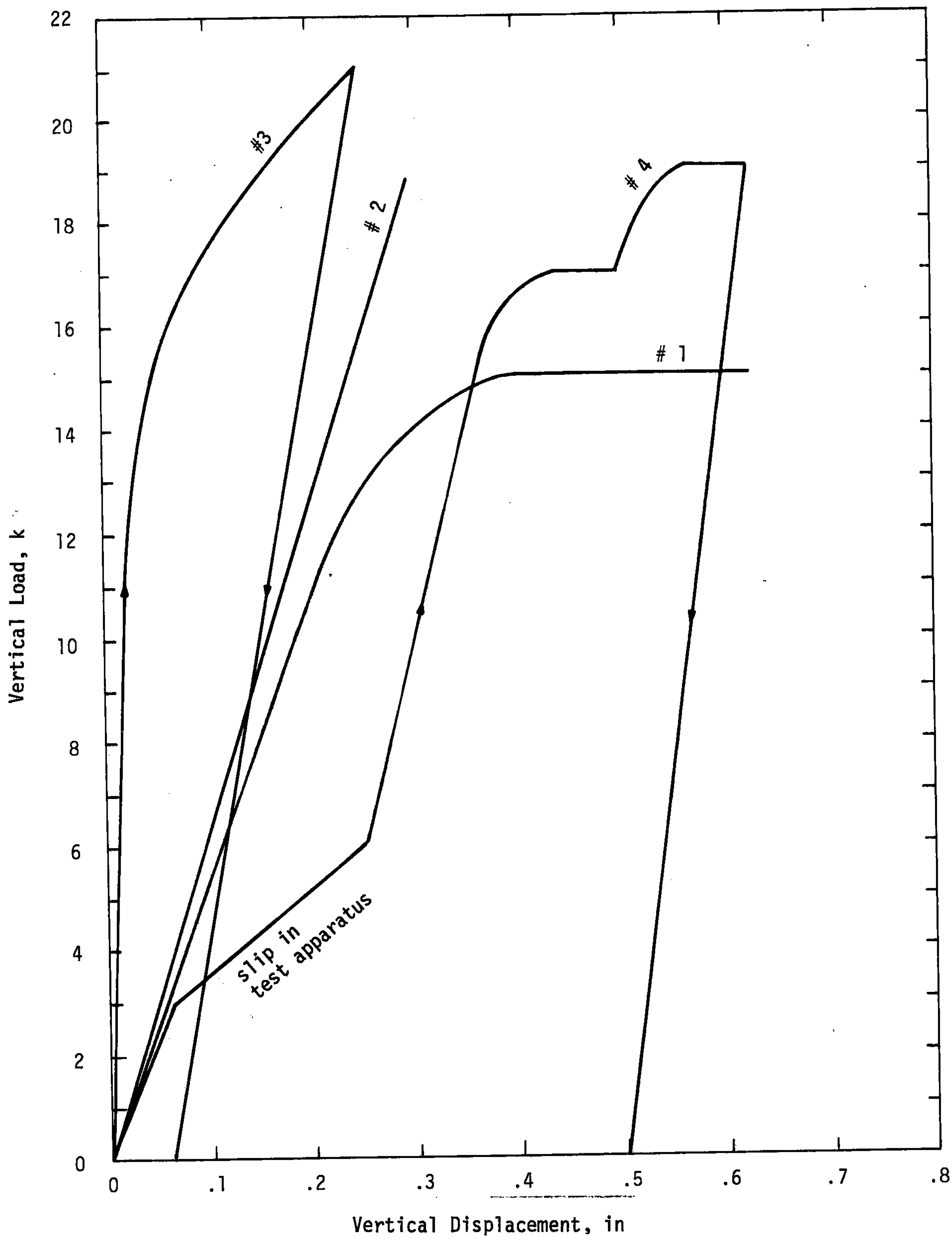

Figure 15. Summary of Vertical Load-Displacement Curves

For the purposes of this report, failure is defined as an obvious break in the load-displacement curve or the load corresponding to a displacement equal to ten percent of the pier diameter. The initial slope is calculated for one-half of the failure load or the maximum applied load, whichever is smaller. The test results are summarized in table 3.

TABLE 3. SUMMARY OF TEST RESULTS

Pier Number	1	2	3	4	5
Horizontal Failure Load, kips	2.5-3.5	7-8	7.25	N/A	4
Horizontal Initial Slope, kips/inch	5	16	10	N/A	35
Vertical Failure Load, kips	15	>19	>21	17-19	Not Tested
Vertical Initial Slope, kips/inch	54	64	263	50	Not Tested

Tension cracks were observed in the soil behind each pier after the applications of the horizontal failure load. Figure 8 shows a typical tension crack. A considerable amount of soil adhered to the surface of the concrete as the piers were removed from the ground, indicating a soil/soil failure rather than a soil/concrete failure. In addition, the entire near-surface block of soil in the square pavement cutout, as well as the surrounding asphalt pavement, were observed to move upward just prior to the onset of large vertical displacements. Figure 9 illustrates this situation just as a circular failure pattern developed in the soil around pier # 1.

Post-test inspections of the piers, which had been removed from the ground, revealed that the concrete had failed at a depth of approximately 32 inches on piers # 2 and 3 and at a depth of 20 inches on pier # 4. No failure crack was observed on pier # 1, but it was impossible to remove all the soil from the pier and a failure crack may have merely remained undetected.

SECTION IV

ANAYLSIS OF RESULTS

The theory developed in Appendix B to reference 1 and the following assumed soil properties were utilized to compute failure loads and to estimate initial horizontal slopes:

$$\text{Wet Density, } \gamma = 118 \text{ pcf}$$

$$\text{Angle of Internal Friction, } \phi = 35 \text{ degrees}$$

$$\text{Cohesion, } C = 1/2\ q_{unfc} = 1500 \text{ psf}$$

The theoretical horizontal failure loads (Q_{um}) are compared with the test results in table 4. It should be noted that the capacity of the reinforced concrete pier governed the failure load in every case and that there is good agreement between these computed capacities and the test results. Considerably more reinforcement would have been required to achieve soil failures. However, the standard pedestal support begins to yield at a load of approximately six kips and the 18 inch diameter reinforced concrete piers have approximately the same capacity. The failure in the reinforced concrete piers was observed to have occurred at approximately the depth of the theoretical maximum moment. After failure of the concrete, additional deflections will occur as a result of rotations about the failure depth.

The theoretical initial horizontal slopes (E_i) are compared with the test results in table 5. The slope of the hystersis loops in figures 11, 12, and 13 are not significantly different from the initial slopes. For the load-unload cycles shown, the permanent set would have been on the order of 0.1 inch or less.

TABLE 4. COMPARISON OF THEORETICAL HORIZONTAL FAILURE LOADS (Q_{um}) WITH TEST RESULTS

Pier Number	1	2	3	4	5
Cohesive Material, kip	4.6	11.4	16.3	7.6	13.7
Cohesionless Material, kip	2.5	9.0	12.5	4.0	7.7
Summation, kip	7.1	20.4	28.8	11.6	21.4
Test Result, kip	2.5-3.5	7-8	7.25	Not Tested	4
Reinforced Concrete Pier Capacity, Kip	3.6	6.7	6.7	3.6	3.6

Note: e = 42"

TABLE 5. COMPARISON OF THEORETICAL INITIAL HORIZONTAL SLOPES WITH TEST RESULTS

Pier Number	1	2	3	4	5
Cohesive Material kip/inch	6	10.2	11.9	Not Tested	10.3
Cohesionless Material kip/inch	1.3	3.1	4.4	"	4.1
Summation kip/inch	7.3	13.3	16.3	"	14.4
Test Result kip/inch	5	16	10	"	35

Notes: e = 42"

$E_i = 1/\delta$ for 1 Kip

The theoretical vertical failure loads (Q_{uv}) are compared with the test results in table 6. There is reasonable agreement for piers # 1 and 4. The vertical load tests on piers # 2 and 3 were stopped far short of their theoretical capacity. Note that pier # 3 was loaded to nearly 50 percent of its theoretical vertical failure load and had a permanent set of less than 0.1 inch. Additional calculations were performed to determine the behavior of the reinforced concrete piers under vertical loads. The applied vertical loads were of insufficient magnitude to have caused a tensile failure of the concrete and the elastic deformations of the reinforcing steel were insignificant compared with the measured displacements.

TABLE 6. COMPARISON OF THEORETICAL VERTICAL FAILURE LOADS (Q_{uv}) WITH TEST RESULTS

Pier Number	1	2	3	4	5
Cohesive Material, kip	10.6	23.0	26.5	13.0	17.1
Cohesionless Material, kip	5.0	15.8	21.0	7.5	13.1
Pier Weight, kip	0.5	1.7	2.0	0.6	0.9
Summation, kip	16.1	40.5	49.5	21.1	31.1
Test Result, kip	15	>19	>21	17-19	Not Tested

It was anticipated that the failure of the soil from the application of an initial horizontal load would result in a significant reduction of the vertical failure load. This was not the case in the observed test results since the reinforced concrete piers failed prior to the failure of the soil.

SECTION V

SUMMARY AND CONCLUSIONS

It appears that all of the reinforced concrete piers in this test failed, rather than the soil, under the application of the eccentric horizontal loads. Therefore, it can only be concluded that the soil had a capacity equal to or larger than the capacity of the reinforced concrete piers. The tensile failure cracks in the concrete occurred at depths approximately equal to the location of the theoretical maximum moment.

The comparison between the theoretical and observed initial horizontal slopes to the load-displacement curves is rather good. The maximum eccentric horizontal load for a typical single-axis-tracking solar collector system is on the order of three kips or less (ref. 2). For maximum loads of this approximate magnitude, the horizontal load-displacement curves display essentially elastic behavior and only minimal permanent sets ($\lesssim$ 0.1 inch) should occur for soils with strengths equal to or greater than the test site.

The theoretical vertical failure loads compared well with the test results, for those piers which did not exceed the capacity of the test apparatus. This suggests that when a material has a cohesion intercept and an angle of internal friction, both parameters should be included in the calculations of failure loads. The minimum test value of 15 kips, for the 12 inch diameter pier, is much greater than the typical maximum vertical load of three kips or less (ref. 2).

The single anchor bolt connection did not perform satisfactorily under the application of horizontal loads and is not recommended for field use. Both the two bolt and four bolt patterns performed well. The typical support pedestal, consisting of a 4 inch x 4 inch x 1/4 inch square post and connection angles, is fairly flexible. A one inch deflection can be expected under the application of a three kip horizontal load with an eccentricity of 42 inches.

Reinforced concrete cylindrical piers are normally the best foundations to support typical single-axis-tracking solar collector systems. The pedestal, pier, soil combination should always be considered in the design process to achieve a balanced design. The theory of Appendix B to reference 1 can be utilized, with appropriate soil parameters, to predict the response of short rigid cylinders subjected to inclined eccentric loads.

With adequately reinforced concrete, the smallest pier in this test series would have carried the maximum expected wind load for a typical system with a factor of safety for the soil greater than three. For soil conditions similar to the test site, the eccentric horizontal failure load (Q_{um}) governs the design and was calculated to be approximately one-half the vertical failure load (Q_{uv}).

REFERENCES

1. Auld, H.E. and Lodde, P.F., Study of Low Cost Foundation Anchor Designs for Single-Axis-Tracking Solar Collector Systems, SAND 78-7048, Sandia Laboratories, Albuquerque, New Mexico, January 1979.

2. Auld, H.E. and Lodde, P.F., Study of Foundation Designs for Single-Axis-Tracking Solar Collector Systems Under Reduced Loading Conditions, Sandia Laboratories, Albuquerque, New Mexico, in publication.

3. Randall, D.E., Standardized Procedure for Estimation of Gross Aerodynamic (Wind) Loads for Single Axis Tracking Parabolic Trough Collectors, unpublished, Sandia Laboratories, Albuquerque, New Mexico, undated.

4. Peck, R.B., Hanson, W.E., and Thornburn, T.H., Foundation Engineering, Second Edition, John Wiley and Sons, Inc., 1974.

5. Subsoil Investigation for Solar Energy Collector Foundations, Kirtland AFB, New Mexico, prepared by F.M. Fox & Associates, Inc., April 23, 1979.

DISTRIBUTION:
TID-4500-R66, UC62 (268)

Aerospace Corporation
101 Continental Blvd.
El Segundo, CA 90245
Attn: Elliott L. Katz

Acurex Aerotherm
485 Clyde Avenue
Mountain View, CA 94042
Attn: H. L. Morse

Argonne National Laboratory (3)
9700 South Cass Avenue
Argonne, IL 60439
Attn: R. G. Matlock
W. W. Schertz
Roland Winston

Barber Nichols Engineering
6325 W. 55th Avenue
Arvada, CO 80002
Attn: R. G. Olander

Battelle Memorial Institute
Pacific Northwest Laboratory
P.O. Box 999
Richland, WA 99352
Attn: K. Drumheller

Congressional Research Service
Library of Congress
Washington, DC 20540
Attn: H. Bullis

Del Manufacturing Co.
905 Monterey Pass Road
Monterey Park, CA 91754
Attn: M. M. Delgado

Desert Research Institute Energy
Systems Laboratory
1500 Buchanan Blvd.
Boulder City, NV 89005
Attn: Jerry O. Bradley

DSET
Black Canyon Stage
P.O. Box 185
Phoenix, AZ 85029
Attn: Gene A. Zerlaut

E-Systems, Inc.
Energy Technology Center
P.O. Box 226118
Dallas, Texas 75266
Attn: Dr. R. R. Walters

Honorable Pete V. Domenici
Room 405
Russell Senate Office Bldg.
Washington, DC 20510

Edison Electric Institute
90 Park Avenue
New York, NY 10016
Attn: L. O. Elsaesser,
Director of Research

Energy Institute
1700 Las Lomas
Albuquerque, NM 87131

EPRI
3412 Hillview Avenue
Palo Alto, CA 94303
Attn: J. E. Bigger

General Atomic
P.O. Box 81608
San Diego, CA 92138
Attn: Alan Schwartz

General Electric Co.
P.O. Box 8661
Philadelphia, PA 19101
Attn: A. J. Poche

Georgia Institute of Technology
Atlanta, GA 30332
Attn: J. D. Walton

Georgia Power Company
Atlanta, GA 30302
Attn: Mr. Walter Hensley
Vice President
Economics Services

Hexcel
11711 Dublin Blvd.
Dublin, CA 94566
Attn: George P. Branch

Jet Propulsion Laboratory
4800 Oak Grove Drive
Pasadena, CA 91103
Attn: V. C. Truscello

Lawrence Berkeley Laboratory
University of California
Berkley, CA 94720
Attn: Mike Wallig

Lawrence Livermore Laboratory
University of California
P.O. Box 808
Livermore, CA 94500
Attn: W. C. Dickinson

DISTRIBUTION (cont)

Los Alamos Scientific Lab. (3)
Los Alamos, NM 87545
Attn: J. D. Balcomb
C. D. Bankston
D. P. Grimmer

Honorable Manuel Lujan
1324 Longworth Building
Washington, DC 20515

Martin Marietta Aerospace
P.O. Box 179
Denver, CO 80201
Attn: R. C. Rozycki

McDonnell-Douglas Astronautics Co.
5301 Bolsa Avenue
Huntington Beach, CA 92647
Attn: Don Steinmeyer

NASA-Lewis Research Center
Cleveland, OH 44135
Attn: R. Hyland

New Mexico State University
Solar Energy Department
Las Cruces, NM 88001

Oak Ridge National Laboratory (2)
P.O. Box Y
Oak Ridge, TN 37830
Attn: S. I. Kaplan
W. R. Mixon

Office of Technology Assessment
U. S. Congress
Washington, DC 20510
Attn: Henry Kelly

Omnium G
1815 Orangethorpe Park
Anaheim, CA 92801
Attn: S. P. Lazzara

PRC Energy Analysis Company
7600 Old Springhouse Road
McLean, VA 22102
Attn: K. T. Cherian

Dr. John D. Reichert
Dept. of Electrical Engineering
Texas Tech University
Lubbock, Texas 79409

Honorable Harold Runnels
1535 Longworth Building
Washington, DC 20515

Honorable Harrison H. Schmitt
Room 1251
Dirksen Senate Office Bldg.
Washington, DC 20510

Scientific Atlanta, Inc.
3845 Pleasantdale Road
Atlanta, Georgia 30340
Attn: A. Ferguson

Solar Energy Research Institute (9)
1536 Cole Blvd
Golden, CO 80401
Attn: B. L. Butler
F. Kreith
C. Grosskreutz
B. P. Gupta
J. Thornton
K. Touryan
N. Woodley
Library (2)

Solar Energy Technology
Rocketdyne Division
6633 Canoga Avenue
Canoga Park, CA 91304
Attn: J. M. Friefeld

Solar Kinetics Inc.
P.O. Box 10764
Dallas, TX 75207
Attn: Gus Hutchison

Southwest Research Institute
P.O. Box 28510
San Antonio, TX 78284
Attn: Danny M. Deffenbaugh

Stanford Research Institute
Menlo Park, CA 94025
Attn: Arthur J. Slemmons

Sun Gas Company
Suite 800, 2 No. Pk. E
Dallas, TX 75231
Attn: R. C. Clark

Sundstrand Electric Power
4747 Harrison Avenue
Rockford, IL 61101
Attn: A. W. Adam

Suntec Systems Inc.
2101 Wooddale Drive
St. Paul, MN 55110
Attn: L. W. Rees

DISTRIBUTION (cont)

Swedlow, Inc.
12122 Western Avenue
Garden Grove, CA 92645
Attn: E. Nixon

U.S. Department of Energy (2)
Agricultural & Industrial
Process Heat
Conservation & Solar Application
Washington, DC 20545
Attn: W. W. Auer
J. Dollard

U.S. Department of Energy (3)
Albuquerque Operationis Office
P.O. Box 5400
Albuquerque, NM 87185
Attn: D. K. Nowlin
G. N. Pappas
W. P. Grace

U.S. Department of Energy
Division of Energy Storage
Systems
Washington, DC 20545
Attn: C. J. Swet

U.S. Department of Energy (8)
Division of Central Solar Technology
Washington, DC 20545
Attn: G. W. Braun
H. Coleman
M. U. Gutstein
G. M. Kaplan
L. Melamed
J. E. Rannels
M. E. Resner
J. Weisiger

U.S. Department of Energy
San Francisco Operations Office
1333 Broadway, Wells Fargo Bldg.
Oakland, CA 94612
Attn: Jack Blasy

University of New Mexico (2)
Department of Mechanical Eng.
Albuquerque, NM 87113
Attn: W. A. Cross
M. W. Wilden

Dr. R. R. Walters
E-Systems Inc.
Energy Technology Center
P.O. Box 22618
Dallas, Texas 75266

Western Control Systems
13640 Silver Lake Drive
Poway, CA 92064
Attn: L. P. Cappiello

Westinghouse Electric Corp.
P.O. Box 10864
Pittsburgh, PA 15236
Attn: J. Buggy

1500 W. A. Gardner
1520 T. L. Pace
1530 W. E. Caldes
1550 F. W. Neilson
1552 O. N. Burchett
2300 J. C. King
Attn: K. L Gillespie, 2320
2323 C. M. Gabriel
2324 L. W. Schulz
2326 G. M. Heck
3161 J. E. Mitchell
3600 R. W. Hunnicutt
Attn: H. H. Pastorius, 3640
3700 J. C. Strassell
4000 A. Narath
4531 J. H. Renken
4700 J. H. Scott
4710 G. E. Brandvold
4713 B. W. Marshall
4714 R. P. Stromberg
4715 R. H. Braasch
4719 D. G. Schueler
4720 V. L. Dugan
4721 J. V. Otts
4722 J. F. Banas (100)
4723 W. P. Schimmel
4725 J. A. Leonard
4725 D. E. Randall
4730 H. M. Stoller
5510 D. B. Hayes
5520 T. B. Lane
5810 R. G. Kepler
5820 R. L. Schwoebel
5830 M. J. Davis
5840 H. J. Saxton
5844 F. P. Gerstle
8100 L. Gutierrez
8124 A. F. Baker
8450 R. C. Wayne
8451 W. G. Wilson
8452 A. C. Skinrood
8453 J. D. Gilson
8266 E. A. Aas
8470 C. S. Selvage
9572 L. G. Rainhart
3141 T. L. Werner (5)
3151 W. L. Garner (3)
For DOE/TIC
(Unlimited Release)

Org.	Bldg.	Name	Rec'd by*	Org.	Bldg.	Name	Rec'd by*

*Recipient must initial on classified documents.